Stable Vortex Tori in the Three-Dimensional Cubic-Quintic Ginzburg-Landau Equation

D. Mihalache,[1,2,3] D. Mazilu,[1,2] F. Lederer,[2] Y. V. Kartashov,[3] L.-C. Crasovan,[3,1] L. Torner,[3] and B. A. Malomed[4]

[1]*Horia Hulubei National Institute for Physics and Nuclear Engineering (IFIN-HH), 407 Atomistilor, Magurele-Bucharest 077125, Romania*

[2]*Institute of Solid State Theory and Theoretical Optics, Friedrich-Schiller Universität Jena, Max-Wien-Platz 1, D-077743 Jena, Germany*

[3]*ICFO—Institut de Ciencies Fotoniques and Universitat Politecnica de Catalunya, Mediterranean Technology Park, 08860 Castelldefels (Barcelona), Spain*

[4]*Department of Interdisciplinary Studies, Faculty of Engineering, Tel Aviv University, Tel Aviv 69978, Israel*

(Received 21 February 2006; published 16 August 2006)

We demonstrate the existence of *stable* toroidal dissipative solitons with the inner phase field in the form of rotating spirals, corresponding to vorticity $S = 0$, 1, and 2, in the complex Ginzburg-Landau equation with the cubic-quintic nonlinearity. The stable solitons easily self-trap from pulses with embedded vorticity. The stability is corroborated by accurate computation of growth rates for perturbation eigenmodes. The results provide the first example of stable vortex tori in a 3D dissipative medium, as well as the first example of higher-order tori (with $S = 2$) in any nonlinear medium. It is found that all stable vortical solitons coexist in a large domain of the parameter space; in smaller regions, there coexist stable solitons with either $S = 0$ and $S = 1$, or $S = 1$ and $S = 2$.

DOI: 10.1103/PhysRevLett.97.073904 PACS numbers: 42.65.Sf, 47.20.Ky

Complex Ginzburg-Landau (CGL) equations have drawn a great deal of attention in physics and applied mathematics communities as a class of universal models with a broad spectrum of applications, ranging from nonlinear optics, fluid dynamics, and chemical waves to second-order phase transitions, including such topics of common interest as superfluidity, superconductivity, liquid crystals, and Bose-Einstein condensates; physical and mathematical aspects of models based on CGL equations were reviewed in Ref. [1]. The CGL equation may be viewed as a dissipative extension of the nonlinear Schrödinger (NLS) equation; accordingly, it can describe a broad range of behaviors suggested by the NLS dynamics, ranging from chaos and pattern formation [2] to *dissipative solitons* [3]. In particular, the latter concept comprises a large variety of phenomena, such as spatial solitons in wide-aperture lasers, ultrashort laser pulses, dispersion-managed solitons in media with loss, filtering, gain, etc. [4,5]. While solitons in conservative systems form continuous families and are supported by the balance between linear effects and nonlinearity, dissipative solitons require an additional balance between linear or nonlinear loss and gain. Thus they do not form continuous families but represent isolated attractors.

Recently, considerable efforts were aimed at the prediction of settings supporting *stable* multidimensional localized patterns. An especially challenging problem is the stabilization of three-dimensional (3D) objects with intrinsic vorticity (*vortex tori*) against both the strong collapse in the 3D space and the well-known splitting instability of localized vortices [6–8]. Thus far, the only prediction of stable 3D vortical solitons was made for ones with vorticity ("spin") $S = 1$, in conservative models that include competing nonlinearities, cubic quintic or quadratic cubic [8]. Remaining outstanding issues are the possibility of finding stable vortex tori with $S > 1$ (which are known in 2D models [7,9]) and the search for stable vortical solitons in dissipative media. In fact, it may be easier to find stable localized vortices in dissipative systems than in their conservative counterparts, as dissipative solitons may be more compact and more robust, and one should not look for a continuous family of solitons but rather for a single attractor shaped as a vortical soliton (for given S). For the same reasons, dissipative spinning 3D solitons may be more relevant to the experiment than their counterparts in conservative models.

The results of Ref. [10], where stable 2D vortex solitons, with a spiral phase field, were found with $S = 1$ and 2, suggest that the complex cubic-quintic Ginzburg-Landau equation may be a relevant model to generate dissipative vortex solitons in the 3D case as well. It is relevant to mention that stable spinless ($S = 0$) 3D solitons were recently found in an optical model based on this equation [11,12]. The objective of the present work is to find stable doughnut-shaped 3D spinning solitons (vortex tori) with $S \geq 1$. The results will yield the first ever example of spinning solitons in a 3D dissipative medium, as well as the first examples of stable *higher-order* ($S > 1$) vortex solitons in *any* 3D model.

We consider a model of a bulk optical medium obeying the following equation with the cubic-quintic nonlinearity:

$$iU_z + \left(\frac{1}{2} - i\beta\right)(U_{xx} + U_{yy}) + (D - i\gamma)U_{tt} + [i\delta + (1 - i\epsilon)|U|^2 - (\nu - i\mu)|U|^4]U = 0. \quad (1)$$

Here U is a local amplitude of the electromagnetic field propagating along the z axis, the coefficients which are scaled to be $1/2$ and 1 account, respectively, for the diffraction in the transverse plane and self-focusing Kerr nonlinearity, $\beta \geq 0$ is an effective diffusivity (the optical model contains the diffusion term if the electromagnetic field generates free carriers, which occurs in semiconductors [10,13] or ionizes the medium, as in the case of the propagation of very strong pulses in air [14]), the positive parameters δ, ϵ, and μ represent linear loss, nonlinear gain, and its saturation, $\nu > 0$ accounts for saturation of the Kerr nonlinearity, D is the group-velocity dispersion (GVD) coefficient, and $\gamma > 0$ is its counterpart accounting for spectral filtering. In cases of anomalous, normal, and zero GVD, D may be normalized to be $1/2$, $-1/2$, or 0, respectively. Below, we set $D = 1/2$. All the physical ingredients included in Eq. (1) come together in the case of the spatiotemporal propagation of light in an active (amplifying) bulk semiconductor featuring saturable absorption.

To construct vortex tori, we look for general solutions to Eq. (1) with a definite value of the above-mentioned vorticity (spin) S, as $U(z, x, y, t) = \Psi(z, r, t)\exp(iS\theta)$, where r and θ are polar coordinates in the plane (x, y). The complex function $\Psi(z, r, t)$ obeys the propagation equation

$$i\Psi_z + \left(\frac{1}{2} - i\beta\right)\left(\Psi_{rr} + \frac{1}{r}\Psi_r - \frac{S^2}{r^2}\Psi\right) + \left(\frac{1}{2} - i\gamma\right)\Psi_{tt} + [i\delta + (1 - i\epsilon)|\Psi|^2 - (\nu - i\mu)|\Psi|^4]\Psi = 0. \quad (2)$$

The solutions Ψ must decay exponentially at r, $|t| \to \infty$, and as $r^{|S|}$ at $r \to 0$.

In direct simulations, we started with an arbitrary axially symmetric input pulse (typically, a Gaussian), with the embedded vorticity S, and simulated Eq. (2) forward in z, expecting that a stable dissipative vortex soliton would self-trap after a certain propagation distance $z = z_f$ into an attractor in the form of $\Psi(z, r, t) = \psi(r, t)\exp(ikz)$, where the propagation constant k is an eigenvalue determined by parameters of Eq. (2), including S (arbitrary pulses with $S = 0$, or, generally, with no definite value of the vorticity, are expected to self-trap into the ordinary isotropic soliton, such as ones studied in Refs. [11,12]). A standard Crank-Nicholson scheme was used for the numerical integration, with typical transverse and longitudinal step sizes $\Delta r = \Delta t = 0.15$ and $\Delta z = 0.01$. Nonlinear finite-difference equations were solved by using the Picard iteration method, and the resulting linear system was handled with the help of the Gauss-Seidel iterative procedure. To achieve good convergence, we typically needed ten Picard and four Gauss-Seidel iterations. The wave number k was determined as the z derivative of the phase of Ψ, and the solution was reckoned to achieve a stationary form if k ceased to depend on z, r, and t, up to five significant digits.

Generic results are adequately represented by the existence and stability domains for spinless and spinning solitons in the parameter plane (μ, ϵ) (see Fig. 1), for fixed $\beta = \gamma = 1/2$, $\nu = 0.1$, and $\delta = 0.4$. In Fig. 1 the solitons

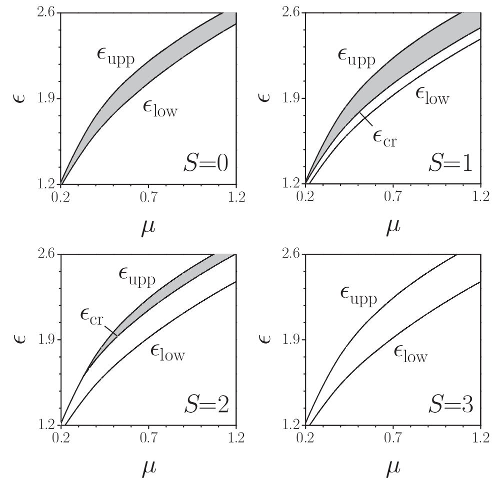

FIG. 1. Domains of the existence and stability of solitons in parameter plane (μ, ϵ), for spin $S = 0$, 1, 2, and 3. The solitons are stable in shaded areas. In this figure and below, other parameters are $\beta = \gamma = 1/2$, $\nu = 0.1$, and $\delta = 0.4$.

exist between curves $\epsilon_{upp}(\mu)$ and $\epsilon_{low}(\mu)$, and they are stable in the shaded portion of this area, which is bounded by a critical line $\epsilon_{cr}(\mu)$, found from the linear stability analysis; see below. Below the curve $\epsilon_{low}(\mu)$, input pulses decay to nil, whereas above the curve $\epsilon_{upp}(\mu)$ they expand indefinitely, generating *fronts* between filled and empty regions. Both the spinning and nonspinning solitons, if stable, are strong attractors, as they self-trap from a large variety of inputs.

Typical radial and temporal cross sections of stable solitons with $S = 0$ and $S = 1$, 2 are displayed in Figs. 2(a)–2(d) for $\mu = 1$ and $\epsilon = 2.44$ (the radial and temporal shapes are shown, respectively, at $t = 0$, and at $r = r_{max}$, where the field attains its maximum). The corresponding wave numbers are $k = 0.689\,26$, $0.736\,91$, and $0.738\,95$, for $S = 0$, 1, and 2, respectively. In particular, panels (c) and (d) demonstrate that, while the temporal shapes of the solitons with $S = 1$ and 2 are virtually identical in terms of $|\psi|$, they are quite different in terms of the real and imaginary parts of the stationary field, ψ_r and ψ_i. The field profiles in Figs. 2(e) and 2(f) are taken from a domain adjacent to the curve ϵ_{upp} separating the stable solitons [ones shown in Figs. 2(a)–2(d)] and indefinitely expanding fronts. These profiles represent, as matter of fact, a new species, *composite 3D solitons*, which feature an essential intrinsic structure in both the radial and temporal directions (their 1D and 2D counterparts were found in Refs. [10,15], respectively).

To study the stability of the stationary solitons in an accurate form, we take a perturbed solution $U = [\psi(r, t) + f(r, t)\exp(\lambda z + iJ\theta) + g^*(r, t)\exp(\lambda^* z - iJ\theta)] \times \exp(ikz + iS\theta)$, where J is an integer azimuthal index of the perturbation, the instability growth rate λ may be complex, and $*$ stands for the complex conjugation (the two components of the perturbation with indices $\pm J$ couple to each other through the nonlinear terms, without

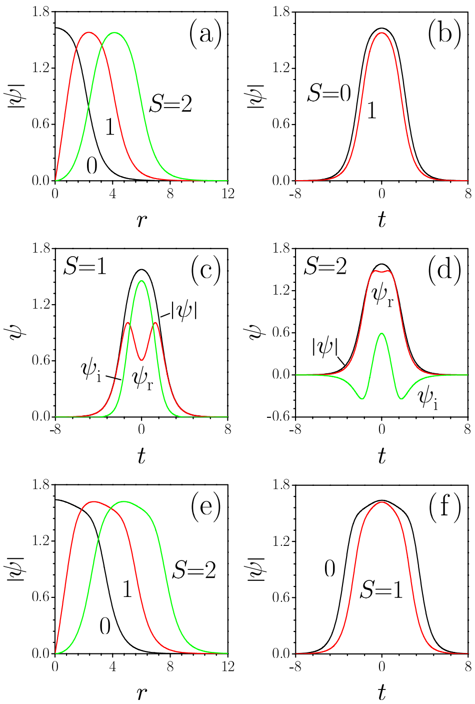

FIG. 2 (color online). Cross-section shapes of typical stable solitons with $S = 0$, $S = 1$, and $S = 2$ in the transverse (r) and temporal (t) directions. Shapes of regular solitons are shown in panels (a)–(d) for $\mu = 1$ and $\epsilon = 2.44$ [in (b), the temporal shape is not shown separately for $S = 2$, as it completely overlaps with that for $S = 1$; real and imaginary parts of the temporal shape for $S = 1$ and $S = 2$ are displayed separately in (c) and (d)]. Panels (e) and (f) display typical shapes of stable *composite solitons*, for $\mu = 1$. Here, $\epsilon = 2.500$ and $k = 0.887\,80$ ($S = 0$), $\epsilon = 2.528$ and $k = 0.905\,08$ ($S = 1$), and $\epsilon = 2.539$ and $k = 0.909\,98$ ($S = 2$).

generating extra angular harmonics). The substitution of the perturbed solution in Eq. (1) leads to linearized equations,

$$(i\lambda + i\delta - k)f + \alpha f_{tt} + \rho\left[f_{rr} + \frac{1}{r}f_r - \frac{(S+J)^2}{r^2}f\right] + 2\eta|\psi|^2 f + \eta\psi^2 g + 3\omega|\psi|^4 f + 2\omega|\psi|^2\psi^2 g = 0, \quad (3)$$

$$(-i\lambda - i\delta - k)g + \alpha^* g_{tt} + \rho^*\left[g_{rr} + \frac{1}{r}g_r - \frac{(S-J)^2}{r^2}g\right] + 2\eta^*|\psi|^2 g + \eta^*(\psi^*)^2 f + 3\omega^*|\psi|^4 g + 2\omega^*|\psi|^2(\psi^*)^2 f = 0, \quad (4)$$

where $\alpha \equiv (1/2 - i\gamma)$, $\rho \equiv 1/2 - i\beta$, $\eta \equiv 1 - i\epsilon$, and $\omega \equiv -\nu + i\mu$. The above equations are supplemented by boundary conditions demanding that the solutions vanish exponentially at r, $|t| \to \infty$, and as $r^{|S\pm J|}$ at $r \to 0$. The Crank-Nicholson method was applied to these equations too, with the same typical transverse and longitudinal step sizes as above, since we had to deal with the same stationary field distributions. The resulting linear algebraic system was solved using a Gauss-Seidel iterative scheme (typically, 25 iterations were sufficient).

The results of the stability calculations are summarized in Fig. 3, where, fixing the quintic loss, $\mu = 1$, we vary the nonlinear gain, ϵ. Panel (a) displays stable and unstable soliton families in terms of the dependence of the total optical energy (alias norm), $E = 2\pi\int_0^\infty r dr \int_{-\infty}^{+\infty} dt|\psi(r,t)|^2$, on ϵ, while other panels specify the (in)stability by showing the largest real parts of the growth rate, Re(λ), vs ϵ. Vertical arrows in Figs. 3(b) and 3(c) mark the left boundary of the stability domain, $\epsilon = \epsilon_{cr}$. It occupies about 70% and 30% of the entire existence domain of the $S = 1$ and $S = 2$ solitons, respectively.

We have also considered the case of $\nu \leq 0$, when the conservative part of Eqs. (1) or (2) would give rise to strong (if $\nu = 0$) or "superstrong" ($\nu < 0$) collapse in the 3D space. The result is that the $S = 0$ soliton family remains stable in this situation, due to the stabilizing effect of the quintic loss. For instance, fixing $\beta = \gamma = 1/2$, $\delta = 0.4$, and $\mu = 1$, the existence and stability region of the solitons with $S = 0$ is found to be $2.336 < \epsilon < 2.500$ for $\nu = +0.1$ (in compliance with Fig. 1), $2.488 < \epsilon < 2.903$ for $\nu = 0$, and $2.630 < \epsilon < 3.451$ for $\nu = -0.1$; i.e., its size actually *increases* for $\nu < 0$, which can be explained. Indeed, while the upper border of this region separates the solitons from the above-mentioned domain-expansion regime, the strong self-focusing, corresponding to $\nu < 0$, counteracts the expansion. We expect that vortical solitons may also be stable for $\nu \leq 0$.

The predictions of the linear stability analysis were verified in direct simulations of Eq. (1). The initial conditions for perturbed solitons were taken as $U(z = 0) = \psi(r,t)(1 + q\phi)\exp(iS\theta)$, where q is a small perturbation amplitude, and ϕ is a random variable uniformly distributed in interval $[-0.5, 0.5]$. We have checked that all the solitons that were predicted above to be linearly stable are

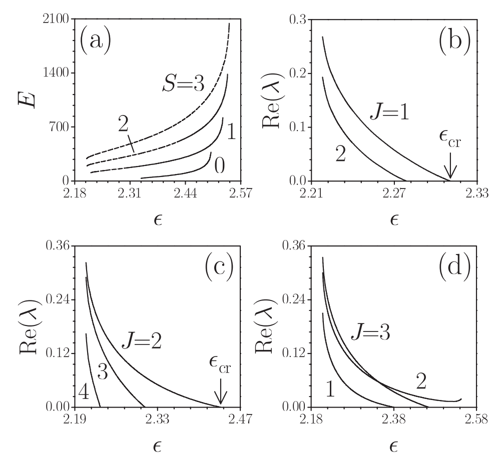

FIG. 3. (a) The soliton's energy (norm) vs the cubic gain ϵ for $\mu = 1$. Solid and dashed lines stand for stable and unstable solitons. Panels (b), (c), and (d) show the largest real part of the perturbation growth rate (eigenvalue) vs ϵ for $S = 1$, $S = 2$, and $S = 3$, respectively.

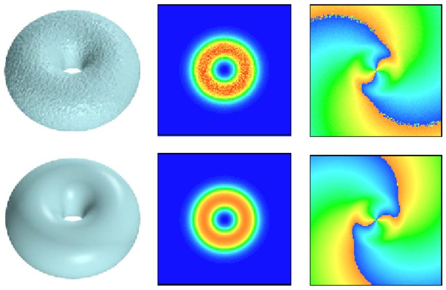

FIG. 4 (color online). The recovery of a perturbed stable soliton with $S = 2$, for $\mu = 1$ and $\epsilon = 2.5$. Upper row: Distribution of intensity ($|U|^2$) and phase in the initial soliton perturbed by random noise. Lower row: The same in the self-cleaned soliton at $z = 800$. The calculations were performed on a grid of size $[-9, 9] \times [-14, 14] \times [-14, 14]$.

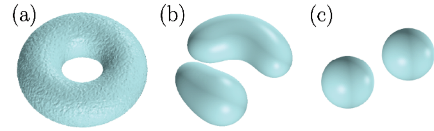

FIG. 5 (color online). Splitting of a perturbed unstable vortex torus with $S = 3$, at $\mu = 1$, and $\epsilon = 2.4$: (a) $z = 0$, (b) $z = 205$, and (c) $z = 500$. The simulations were performed on a grid of size $[-9, 9] \times [-15, 15] \times [-15, 15]$.

indeed stable against finite random perturbations. An example of self-healing of the $S = 2$ stable soliton, with the initial perturbation amplitude at the 10% level, is displayed in Fig. 4. On the other hand, those spinning solitons, which were predicted to be unstable, either decay or split into spinless solitons, if slightly perturbed. A typical example of the splitting of a $S = 3$ soliton into two pulses with $S = 0$ due to the azimuthal instability is shown in Figs. 5(a)–5(c). The outcome agrees with the fact that, since Fig. 3(d) predicts the strongest instability mode for this soliton with $J = 2$, it should indeed split into two fragments.

In conclusion, we have systematically analyzed the existence and stability of 3D spinless and spinning dissipative solitons in the framework of the complex Ginzburg-Landau equation with the cubic-quintic nonlinearity. The stability of solitons with spin 0, 1, and 2 against both small and large perturbations and their propensity to self-trapping from a broad class of input pulses with embedded vorticity have been demonstrated. All the stable solitons coexist in a large domain of the parameter space, each being a strong attractor inside its own class of initial conditions, distinguished by the vorticity. We conjecture that the solitons with $S > 2$ may also be stable, but in very small parameter regions, as suggested by known results for the stability of vortex solitons with $S \geq 3$ in the 2D NLS equation with the cubic-quintic nonlinearity [9]. The stability of the 3D solitons was also demonstrated in the case when the quintic term in the conservative part of the model tends to initiate superstrong collapse.

The results reported in this Letter provide the first example of stable higher-order vortex tori (with $S = 2$) and also the first example of any stable vortex solitons in a 3D dissipative medium. These results, obtained in the paradigmatic complex cubic-quintic Ginzburg-Landau model, suggest that similar stable localized objects with intrinsic vorticity may also be found in more complex 3D dissipative models, such as ones describing the transmission of very strong laser pulses in air (in that case, the propagation equation for the electromagnetic wave is coupled to a kinetic equation accounting for the generation of plasma). In the latter case, the first results of direct simulations show that vortical pulses can be created, but they split due to the azimuthal instability [16]; nevertheless, our predictions here suggest that stabilization might occur if propagation conditions that may be approximately modeled by a three-dimensional complex cubic-quintic Ginzburg-Landau equation are identified.

This work was supported in part by DFG, Bonn (Germany) and by the Ramón y Cajal and Juan de la Cierva programmes.

[1] I. S. Aranson and L. Kramer, Rev. Mod. Phys. **74**, 99 (2002); B. A. Malomed, in *Encyclopedia of Nonlinear Science*, edited by A. Scott (Routledge, New York, 2005), p. 157.

[2] M. C. Cross and P. C. Hohenberg, Rev. Mod. Phys. **65**, 851 (1993); P. Mandel and M. Tlidi, J. Opt. B **6**, R60 (2004).

[3] *Dissipative Solitons*, edited by N. Akhmediev and A. Ankiewicz, Lecture Notes in Physics Vol. 661 (Springer, Berlin, 2005).

[4] S. Barland *et al.*, Nature (London) **419**, 699 (2002); Z. Bakonyi *et al.*, J. Opt. Soc. Am. B **19**, 487 (2002); E. A. Ultanir *et al.*, Phys. Rev. Lett. **90**, 253903 (2003).

[5] B. A. Malomed, *Soliton Management in Periodic Systems* (Springer, New York, 2006).

[6] A. S. Desyatnikov, Y. S. Kivshar, and L. Torner, Prog. Opt. **47**, 291 (2005).

[7] B. A. Malomed *et al.*, J. Opt. B **7**, R53 (2005).

[8] D. Mihalache *et al.*, Phys. Rev. Lett. **88**, 073902 (2002); Phys. Rev. E **66**, 016613 (2002).

[9] R. L. Pego and H. A. Warchall, J. Nonlinear Sci. **12**, 347 (2002).

[10] L.-C. Crasovan, B. A. Malomed, and D. Mihalache, Phys. Rev. E **63**, 016605 (2001); Phys. Lett. A **289**, 59 (2001).

[11] P. Grelu, J. M. Soto-Crespo, and N. Akhmediev, Opt. Express **13**, 9352 (2005); J. M. Soto-Crespo, P. Grelu, and N. Akhmediev, Opt. Express **14**, 4013 (2006).

[12] V. Skarka and N. B. Aleksić, Phys. Rev. Lett. **96**, 013903 (2006).

[13] H. Sakaguchi and B. A. Malomed, Physica (Amsterdam) **167D**, 123 (2002).

[14] S. Skupin *et al.*, Phys. Rev. E **70**, 046602 (2004).

[15] V. V. Afanasjev, N. Akhmediev, and J. M. Soto-Crespo, Phys. Rev. E **53**, 1931 (1996).

[16] A. Vinçotte and L. Bergé, Phys. Rev. Lett. **95**, 193901 (2005).